Journal of Structural Geology, Vol. 11, No. 5, pp. 613 to 623, 1989
Printed in Great Britain

0191-8141/89 $03.00 + 0.00

Crystal rotation by mechanical interaction between plastically anisotropic crystals

THOMAS M. THARP

Department of Earth and Atmospheric Sciences, Purdue University, West Lafayette, IN 47907, U.S.A.

(*Received* 30 *November* 1987; *accepted in revised form* 21 *December* 1988)

Abstract—In polycrystalline material, minerals with pronounced plastic anisotropy may experience inhomogeneous deformation and significant mechanical interaction between neighboring crystals. To study the effect of crystal interaction on preferred orientation, pure shear of a polycrystalline material with identical, orthogonal slip systems was modeled two-dimensionally by the finite-element method. Such a material is non-ductile in the formal von Mises sense because it lacks five independent slip systems. As a result, each crystal has highly anisotropic strength. Because a homogeneous, irrotational strain history in a two-dimensional crystal with identical, orthogonal slip systems does not cause lattice rotation, rotation caused by crystal interaction is readily observed. In the finite-element models, slip planes rotate toward a preferred orientation parallel to maximum shear stress (45° to shortening and extension directions). Mechanical interaction between neighboring crystals produces this preferred orientation by rigid-body rotation of crystals or parts of crystals not favorably oriented for slip.

INTRODUCTION

MOST previous analyses of preferred orientation fabrics have assumed that crystals do not interact. The non-interacting crystal models that are most useful, and that are referred to in this paper, assume that each crystal in a polycrystalline material experiences the same strain (e.g. Taylor 1938, Lister *et al.* 1978). With this assumption, the dominant slip plane will rotate until it is normal to the axis of greatest shortening. If there are multiple slip systems with similar critical resolved shear stress, crystal axes will rotate to facilitate multiple slip in rotationally stable orientations (Lister *et al.* 1978, Lister & Paterson 1979, Lister & Williams 1979, Lister & Hobbs 1980, Wagner *et al.* 1982, 1984). These models for preferred orientation of non-interacting crystals should be most accurate when strain is homogeneous (as assumed in the models cited above) or when unequally deformed grains can slip past one another (Etchecopar 1977). The models are in good agreement with observed fabrics in both naturally and experimentally deformed quartz (e.g. Tullis *et al.* 1973, Bouchez 1977, Law *et al.* 1984, Price 1985, Law 1986) and calcite (e.g. Knopf 1949, Turner & Ch'ih 1951, Wenk *et al.* 1973, Rutter & Rusbridge 1977, Wagner *et al.* 1982, Wenk *et al.* 1986a,b, Takeshita *et al.* 1987); however, the models may not accurately characterize simple shear in quartz (Schmid & Casey 1986) nor pure axial deformation in calcite (Wenk *et al.* 1986a).

Numerical models by Gotoh (1978) and Lin (1964) account for crystal interaction; but Gotoh investigated a formally ductile material (one with five independent slip systems) and did not investigate development of preferred orientation, and because Lin's analysis considered only infinitesimal strains, it pertains to neither large strains nor development of preferred orientation. Numerical models by Etchecopar (1977) and Etchecopar & Vasseur (1987) allow some crystal interaction, but require homogeneous strain within crystals and do not maintain continuity at grain boundaries. The finite-element models described below preserve grain-boundary continuity and model the effect of crystal interactions on preferred orientation for large, geologically significant strains.

A material that is non-ductile in the von Mises sense was chosen for study because it represents an extreme case of plastic anisotropy. I shall review the implications and limitations of the von Mises ductility criterion and demonstrate that, for plane strain, two orthogonal slip systems do not allow ductility in this restricted sense. I then show that a material with identical orthogonal slip systems will not experience crystal lattice rotation when subjected to an irrotational strain history. The finite-element model is then discussed, followed by discussion of the results.

VON MISES DUCTILITY

For a polycrystalline material to be ductile in the sense defined by von Mises (1928), its constituent crystals must be able to undergo an arbitrary plastic strain (Nicolas & Poirier 1976). This condition allows any state of plastic strain in a crystal to be accommodated by plastic strain in adjacent crystals. In the absence of this condition, distortion of a crystal by plastic strain cannot be wholly accommodated by plastic strain in adjacent crystals. This distortion must therefore be accommodated in part by elastic strain in adjacent crystals, except for special crystal shapes and strain geometries (Kocks & Canova 1981). It is convenient in this paper to define formal ductility in the restricted sense defined by von Mises. The von Mises ductility criterion is useful in distinguishing ductile from brittle materials; however some

formally non-ductile materials (e.g. calcite at low temperature and shear stress too low for *r* glide) undergo large strains by inhomogeneous deformation at the crystal level, without brittle failure. For this reason, the formal von Mises definition of ductility is distinguished from the common observational definition.

Most rock-forming minerals are formally non-ductile at low temperature (Paterson 1969, Nicolas & Poirier 1976). Even when they undergo large strains at higher temperature, their low symmetry dictates that most plastic strain will occur on one or a few slip systems, at low resolved shear stress. Strain components not allowed by these slip systems are accommodated by inhomogeneous deformation and elastic strain in the finite-element models described in this paper. In real crystals, at metamorphic or higher temperatures, these strains are also accommodated by glide on slip systems requiring higher resolved shear stress, and by other inelastic processes such as climb, Nabarro–Herring creep and Coble creep.

Conditions for formal (von Mises) ductility

It was shown by von Mises (1928) and Bishop (1953) that a crystalline material must have five independent slip systems to experience an arbitrary infinitesimal strain increment by slip, and this criterion defines formal ductility. A slip system is defined by a family of parallel crystallographic planes on which slip occurs, and by the direction of slip on those planes (Nicolas & Poirier 1976). Groves & Kelly (1963) defined a slip system by the unit vector **n** normal to the slip plane:

$$\mathbf{n} = n_x\mathbf{i} + n_y\mathbf{j} + n_z\mathbf{k} \tag{1}$$

and the unit vector **b** in the direction of the Burgers vector:

$$\mathbf{b} = b_x\mathbf{i} + b_y\mathbf{j} + b_z\mathbf{k}, \tag{2}$$

where the x, y, z co-ordinate system is fixed in relation to the crystallographic co-ordinate system (Tharp 1985a). The infinitesimal strain components caused by a single slip system are:

$$\begin{aligned} \varepsilon_x &= \alpha n_x b_x \quad \varepsilon_y = \alpha n_y b_y \quad \varepsilon_z = \alpha n_z b_z \\ \varepsilon_{xy} &= (\alpha/2)(n_x b_y + n_y b_x) \\ \varepsilon_{xz} &= (\alpha/2)(n_x b_z + n_z b_x) \\ \varepsilon_{yz} &= (\alpha/2)(n_y b_z + n_z b_y), \end{aligned} \tag{3}$$

where α is shear strain in the plane of the slip system. Groves & Kelly (1963) developed a procedure for demonstrating independence of five slip systems and therefore ductility for infinitesimal strain. Magnitude and sign of α are arbitrary for the ductility analysis as long as magnitude is not zero. Although there are six strain components, only five are independent, because for deformation by slip alone, the sum of the normal strains is zero; i.e. volume is constant. This independence of five slip systems is established if the determinant of a 5 × 5 matrix of strain components is non-zero (Groves & Kelly 1963).

Conditions for formal ductility in plane strain

The two-dimensional, plane strain ductility condition is derived from the general three-dimensional condition. A slip system is defined for the two-dimensional case (Fig. 1) by a unit vector **n** normal to the slip plane and a unit vector **b** parallel to the Burgers vector:

$$\begin{aligned} \mathbf{n} &= n_x\mathbf{i} + n_y\mathbf{j} = -\sin\theta\mathbf{i} + \cos\theta\mathbf{j} \\ \mathbf{b} &= b_x\mathbf{i} + b_y\mathbf{j} = \cos\theta\mathbf{i} + \sin\theta\mathbf{j}, \end{aligned} \tag{4}$$

where θ is the counterclockwise angle between the x-axis and the slip plane (Fig. 1). If α is set to 1.0, for convenience, the three non-zero strain components are:

$$\begin{aligned} \varepsilon_x &= n_x b_x = -\sin\theta\cos\theta \\ \varepsilon_y &= n_y b_y = \cos\theta\sin\theta \\ \varepsilon_{xy} &= (1/2)(n_x b_y + n_y b_x) = (1/2)(-\sin^2\theta + \cos^2\theta). \end{aligned}$$

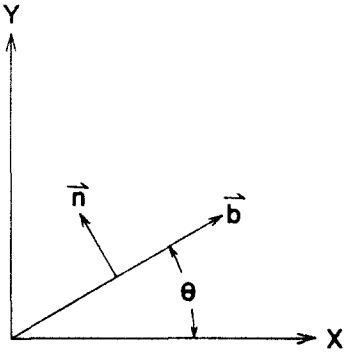

Fig. 1. Definition of slip system geometry for plane strain; **n** is the normal to the slip plane and **b** is the direction of slip.

For strain by slip alone $\varepsilon_x + \varepsilon_y = 0$, and therefore there are only two independent strains. Thus, the 5 × 5 matrix for the three-dimensional case is reduced to the 2 × 2 matrix $[A]$:

$$[A] = \begin{bmatrix} (\varepsilon_x - \varepsilon_y)_1 & \varepsilon_{xy1} \\ (\varepsilon_x - \varepsilon_y)_2 & \varepsilon_{xy2} \end{bmatrix} = \begin{bmatrix} -2\sin\theta_1\cos\theta_1 & (1/2)(\cos^2\theta_1 - \sin^2\theta_1) \\ -2\sin\theta_2\cos\theta_2 & (1/2)(\cos^2\theta_2 - \sin^2\theta_2) \end{bmatrix},$$

where θ_1 and θ_2 pertain to two different slip systems. The determinant of $[A]$ is:

$$\begin{aligned} \text{Det}\,[A] = &-\sin\theta_1\cos\theta_1(\cos^2\theta_2 - \sin^2\theta_2) \\ &+ \sin\theta_2\cos\theta_2(\cos^2\theta_1 - \sin^2\theta_1). \end{aligned}$$

The conditions for which two slip systems fail to provide ductility are found by setting Det $[A]$ to zero. This relationship is satisfied if $\theta_1 = \theta_2 + 90°$, i.e. the two slip systems are orthogonal. Thus, a material with only two orthogonal slip systems is formally non-ductile. That such a material is non-ductile is easily seen. For orthogonal slip systems parallel to the x and y co-ordinate axes ε_{xy} can be accommodated, but clearly no slip on either slip system can produce ε_x or ε_y.

ROTATION

It can also be demonstrated that any stress applied to identical orthogonal slip systems will produce strain without crystal lattice rotation. Figure 2 shows two orthogonal slip systems with normals and slip directions defined so that for any state of stress the crystal lattice on the $+\mathbf{n}$ side of the slip plane will move in the $+\mathbf{b}$ direction for both slip systems or in the $-\mathbf{b}$ direction for both slip systems. Strains in x–y co-ordinates for shear strain α on a slip system are defined by equations (1)–(3). For slip system 1,

$$\mathbf{n}_1 = -\sin\theta\mathbf{i} + \cos\theta\mathbf{j}$$
$$\mathbf{b}_1 = \cos\theta\mathbf{i} + \sin\theta\mathbf{j}.$$

Substitution of the vector coefficients into equations (3) yields, for the non-zero strain components:

$$\varepsilon_{x1} = -\alpha\sin\theta\cos\theta$$
$$\varepsilon_{y1} = \alpha\cos\theta\sin\theta$$
$$\varepsilon_{xy1} = (\alpha/2)(-\sin^2\theta + \cos^2\theta).$$

For slip system 2,

$$\mathbf{n}_2 = \cos\theta\mathbf{i} + \sin\theta\mathbf{j}$$
$$\mathbf{b}_2 = -\sin\theta\mathbf{i} + \cos\theta\mathbf{j}.$$

Substitution of the vector coefficients for slip system 2 into equations (3) yields the same strain components produced by slip system 1. Slip on any slip system produces simple shear. Although the crystal lattice is not rotated by simple shear, simple shear is the sum of a pure shear (shear strain) and a rotation of the mass of the crystal. This rotation ω_{xy} caused by the slip (Lister *et al.* 1978, Van Houtte & Wagner 1985) is:

$$\omega_{xy} = (\alpha/2)(n_x b_y - n_y b_x). \quad (5)$$

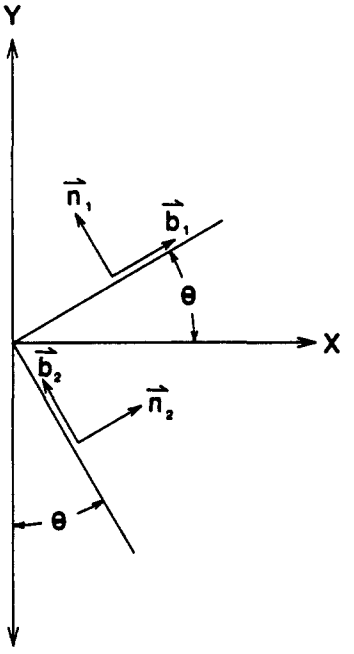

Fig. 2. Normal vectors $\mathbf{n}_1$ and $\mathbf{n}_2$ and slip direction vectors $\mathbf{b}_1$ and $\mathbf{b}_2$ for orthogonal slip systems.

For slip system 1, $\omega_{xy} = -\alpha/2$ and for slip system 2, $\omega_{xy} = \alpha/2$. That is, for a given α, the two orthogonal systems produce opposite rotations of equal magnitude. For static equilibrium, shear stress must always be equal on orthogonal planes (Timoshenko & Goodier 1970, p. 5). Because shear stress on the identical, orthogonal slip systems is equal, they must always experience the same strain α, causing rotations to cancel.

If the deformation gradient (Van Houtte & Wagner 1985) imposed on a crystal is irrotational, (i.e. strains without rigid-body rotations), the crystal mass must be free of rotation following slip. This requires an additional rigid-body rotation of the crystal that is equal in magnitude and opposite in direction to the rotation described above that results directly from slip (Lister *et al.* 1978, Van Houtte & Wagner 1985). This compensating rotation rotates the crystal lattice and is the cause of the preferred orientation computed for non-interacting crystal models. Because the rotations ω_{xy} for the two orthogonal slip systems cancel, the compensating lattice rotations also cancel. Thus, for identical, orthogonal slip systems, net lattice rotations are zero for non-interacting crystals undergoing homogeneous, irrotational strain. For non-interacting crystals of this type, any pre-existing distribution of crystal orientations is therefore stable and no new preferred orientation will develop.

FINITE-ELEMENT MODELS

The two-dimensional plane strain program (Tharp 1985b) employs 8-node isoparametric elements. Displacement within an element and on its boundaries is quadratic, as defined by displacement of the nodes. This guarantees strain compatibility both within elements and at boundaries between elements. Orthogonal slip systems in each element are modeled by a plastic yield condition which specifies that shear stress cannot exceed the yield stress τ_f on planes of a particular orientation. Because $\tau_{xy} = \tau_{yx}$ (Timoshenko & Goodier 1970, p. 5), this condition applies to an orthogonal plane as well. Thus, specification of one slip system in the finite-element model automatically engenders a second, orthogonal slip system with identical properties. Identical orthogonal slip systems defined in this way are not only ideal for the purposes of the present study, but they also probably represent the only slip system configuration definable in a standard finite-element program. Definition of a single slip system or of non-orthogonal slip systems requires special finite-element formulations (Gotoh 1978, Dafalias 1984, Needleman *et al.* 1985).

Poisson's ratio is 0.2 in all analyses and, unless otherwise stated, $\tau_f/G = 2.4 \times 10^{-3}$, where G is shear modulus. The orthotropic elastic constants (Zienkiewicz 1971, p. 55) of each element are referred to co-ordinates x' and y', parallel and perpendicular to the slip plane. Young's modulus E' and Poisson's ratio ν' are the same

in the x' and y' directions, and shear modulus G' is initially set equal to the isotropic elastic shear modulus $G = E'/2(1 + \nu')$, making the element isotropic in the elastic range.

Vertical displacements are imposed on the upper and lower boundaries of the mesh in 10 equal increments, with total shortening in the vertical direction of 40% in all runs. Because horizontal displacements are imposed to preserve constant volume, the resulting strain is pure shear. For each displacement increment, element constitutive properties are adjusted iteratively until each plastically deformed element satisfies the yield condition at the Gauss points. When yield stress on the slip plane is exceeded at a Gauss point, the effective shear modulus G' is reduced for the next iteration to a value that would make shear stress equal to τ_f for the computed shear strain on the slip plane. Only a few iterations are generally required to closely satisfy the yield condition.

Slip system (crystal lattice) orientation is initially constant within each element. Before each displacement increment the nodal co-ordinates are adjusted to reflect cumulative displacement. New slip system orientations are also calculated at each Gauss point to reflect the change in attitude caused by rotation. In this way, large finite strains and rotations of elements and slip systems accumulate in a series of smaller increments.

The finite-element meshes are initially square and composed of 36 elements (e.g. Fig. 3). The line segments shown in each element represent the attitude of one of the slip planes at each of the nine Gauss points used in the finite-element calculations; the other slip plane is always orthogonal to the one shown. Only one of the orthogonal slip planes is depicted, to make the sense of rotation between initial and final states more apparent.

In the finite-element models each element is considered a single crystal. Initial slip system orientations were produced by a random number generator, but orientations were restricted in some cases to produce an initial preferred orientation. Because imposed displacements are symmetrical about the vertical axis (shortening direction), the sets of orientations to be used were screened to ensure that slip systems of low (or high) dip have no strong preferred dip orientation to either the right or left of vertical.

DEFORMATION BEHAVIOR

Figures 3 and 4 show the undeformed mesh, deformed mesh and final stress state for an initially random distribution of slip system orientations (Fig. 3), and for slip systems with initial preferred orientations nearly

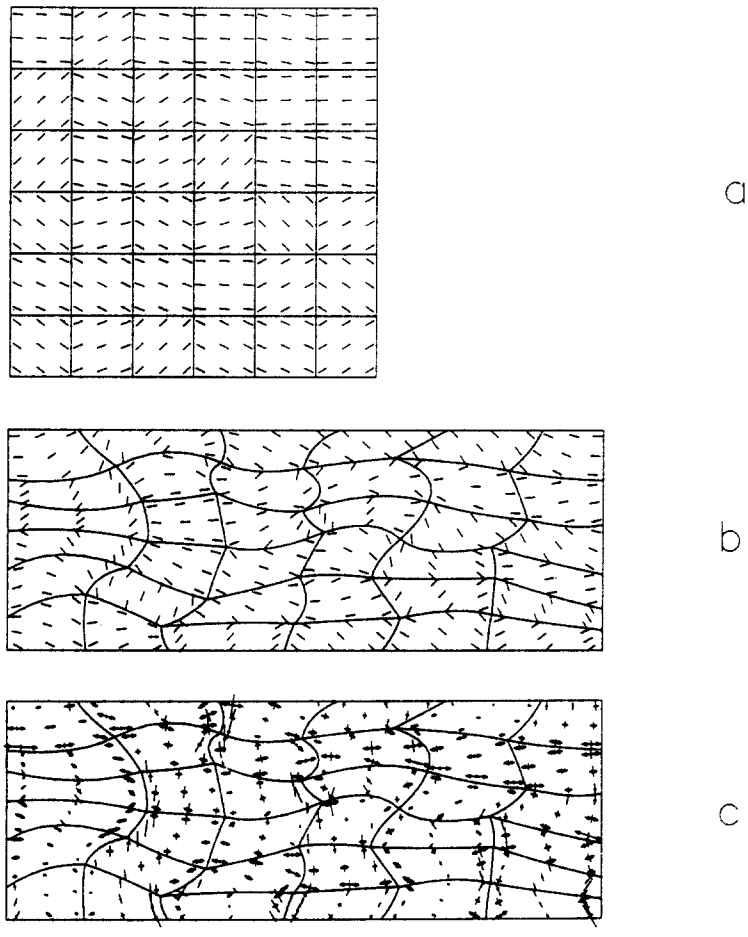

Fig. 3. (a) Undeformed finite-element mesh showing slip plane orientations at Gauss points. Slip plane orientations are random (uniformly distributed over all orientations) but only the shallow-dipping slip plane (−45° to +45°) is shown for each orthogonal pair. (b) Deformed mesh after 40% strain. (c) Stress state after 40% strain; bars with arrow heads indicate tension, solid bars compression, length of bar is proportional to stress magnitude.

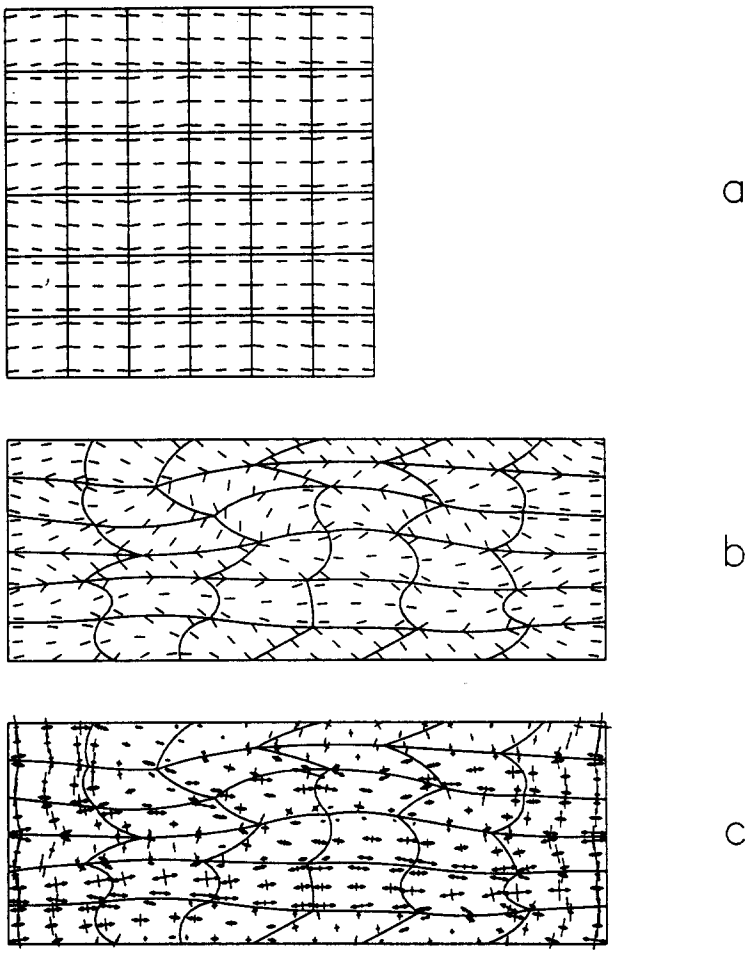

Fig. 4. (a) Undeformed finite-element mesh. The mean dip for the shallow-dipping slip plane of the orthogonal pairs is 5°, and thus the mean dip of the more steeply dipping of the pairs is 85°. Only the shallow-dipping slip plane is shown. (b) Deformed mesh after 40% strain. (c) Stress state after 40% strain; bars with arrow heads indicate tension, solid bars compression, length of bar is proportional to stress magnitude.

horizontal and vertical (Fig. 4). In Fig. 4, the mean absolute value of inclination from the horizontal of the flatter-dipping slip planes was initially 5°; therefore, the mean absolute value of inclination from the horizontal of the steeper dipping of each orthogonal pair was 85°. Although the mean absolute value of inclinations is 5° for the flatter dipping set, the orientations of this set cluster about zero, reflecting the equality of dips to left (+) and right (−). The orientations of the steeper dipping set cluster about 90°. Only the initially flatter dipping of each pair of slip planes is shown in Figs. 3 and 4.

Strain is extremely inhomogeneous (Figs. 3 and 4), as expected in deformation of a formally non-ductile material. Crystal lattices rotate both clockwise and counterclockwise, locally by large angles. Final stress states (Figs. 3c and 4c) are also inhomogeneous, particularly in the center of the mesh, where boundary constraint effects are less important. Principal stress directions in individual crystals depart significantly from the horizontal tension and vertical compression of a homogeneous, isotropic material.

Deformation in models with orthogonal slip systems is both elastic and plastic, with inhomogeneous distribution of the two mechanisms between and within crystals. Orientation of an element and the stress state imposed by surrounding elements may dictate that parts of an element deform almost entirely by plastic strain, while elastic strain dominates in other parts. At any location, shear strain parallel to slip systems will be almost entirely plastic, because for $\tau_f/G = 2.4 \times 10^{-3}$, maximum elastic shear strain in those orientations is 2.4×10^{-3}, very small relative to 40% compression. However, because normal stresses parallel or perpendicular to the slip systems may become arbitrarily high without triggering slip, possible elastic strains in those two directions are unlimited. As will be discussed in a later paper, for large strain in these finite-element models, approximately 1/4 of total strain is elastic. This allows convergence and divergence of slip plane orientations within a crystal, and length change parallel to slip planes; phenomena that in real crystals would be partially accommodated by kinking, minor slip on slip systems with higher critical resolved shear stress, or by non-plastic deformation mechanisms.

Figures 3 and 4 illustrate some important features of finite strain with identical, orthogonal slip systems. Because homogeneous strain does not cause crystal lattice rotation, the rotations reflect local rigid-body

rotation caused by inhomogeneous deformation. This is well illustrated in the lowest row of elements in Fig. 4(b), where two elements have experienced a large component of simple shear. This could be accommodated by glide on the nearly horizontal slip plane without net lattice rotation. However, because the two orthogonal slip systems in each element are identical and experience the same shear stress, they must also undergo identical slip. As established above, the irrotational component of deformation produces no lattice rotation. The observed lattice rotation therefore results from the rigid-body rotational component of the simple shear to which the elements have been subjected. Because simple shear has rotated these slip planes into orientations favorable to slip (oblique to principal strains in the body as a whole), later strain has allowed flattening of these elements without significant additional rotation. This late strain episode is indicated by the small magnitude of stresses in the final state (Fig. 4c). These crystals would, of course, behave differently if they had only a single slip system rather than orthogonal slip systems. The observed simple shear would result in lattice rotation if the high angle slip plane alone were present, but no lattice rotation would occur if the nearly horizontal slip plane alone were present.

Although deformational behavior is strongly a function of the slip and twin systems available in a particular mineral, the finite-element models share a number of characteristics with naturally and experimentally deformed monomineralic rocks. Inhomogeneity of strain is difficult to document in rocks because grains in the undeformed state differ in size and shape; however, the presence of undeformed or weakly deformed quartz grains in the midst of strongly deformed grains has been noted by Tullis *et al.* (1973), Mancktelow (1981) and Law (1986). As in the finite-element models, the weakly deformed grains are unfavorably oriented for slip. It is also noted that such undeformed grains are observed only where the strain history is irrotational. This suggests that for deformation gradients (Van Houtte & Wagner 1985) with a large component of rigid-body rotation, unfavorably oriented grains are eventually rotated into orientations favorable for slip.

Inhomogeneous deformation is also common within individual grains in naturally and experimentally deformed rock. Undulatory extinction grades into optically distinguishable subgrains with orientation mismatches of up to 10° or 15°. At higher strains, original grains may be surrounded by subgrains, with misorientation increasing away from the center of the original grain (Urai *et al.* 1986). With sufficient strain, this progressive rotation of subgrains produces high-angle grain boundaries and a 'recrystallized' texture. Similar rotations occur in the finite-element models, but the rotation gradients are smooth rather than being expressed as discrete rotations across grain or subgrain boundaries, and the boundaries of original crystals remain known, rather than being lost in the mass of small reoriented grains between the remnants of original grains.

PREFERRED ORIENTATION OF SLIP SYSTEMS

Figure 5 shows distributions of initial and final slip plane orientations at Gauss points and net change in orientation for models with different initial slip system orientations. The histograms are means of slip plane histograms for three separate finite-element models, except the histogram for initial mean orientations of 20° and 70°, which was calculated from six separate models. For all initial orientations, the result of 40% vertical shortening is an increase in slip planes oriented 45° from the direction (horizontal) of maximum extension. This orientation produces the highest resolved shear stress on the orthogonal slip planes and is, therefore, the orientation most favorable for slip. The peak at 45° is subdued, but it is also found in each of the many finite-element models individually.

The 45° preferred orientation means that the two slip systems tend to be symmetrically disposed about the shortening direction, as would be expected for a non-interacting crystal model for lattice rotation. As shown above, however, for identical, orthogonal slip systems no crystal lattice rotation would occur if the crystals were non-interacting.

The preferred orientation observed in the finite-element models must therefore be caused by crystal interaction. Although crystal interactions are not easily understood, the following explanation seems consistent with observed deformation in many individual elements and groups of elements. In the finite-element models, both plastic strains and local rigid-body rotations are large. A crystal, or part of a crystal, with orientation unfavorable to slip in the local stress field is required by grain-boundary continuity to rotate rigidly as adjacent crystals deform. When it has rotated into a position favorable to slip, shear occurs. Because boundary displacements imposed by strain in neighboring crystals can then be accommodated by slip on the orthogonal slip systems rather than by rotation, and because slip does not produce rotation in these models, the rate of rigid-body rotation decreases. Therefore, orientations favorable to shear tend to be most stable, and are preserved.

Although persistence of orientations favorable to shear is attributable to the existence of orthogonal slip systems, other aspects of the suggested model should apply to other materials as well. When a crystal's orientation does not allow slip in the local stress field, compatibility with neighboring crystals can be maintained, in part, by local rigid-body rotation. Because non-slip orientations experience rigid-body rotation in place of strain, their orientation is unstable. The rotations imposed are unrelated to crystallographic orientation, but because only non-slipping crystals are required to rotate in this way to maintain strain compatibility, this behavior will produce a net rotation toward orientations favorable to slip. This process should occur to varying degrees in many, and perhaps all, polycrystalline materials, although its effect will be partially masked in most by lattice rotations associated with slip.

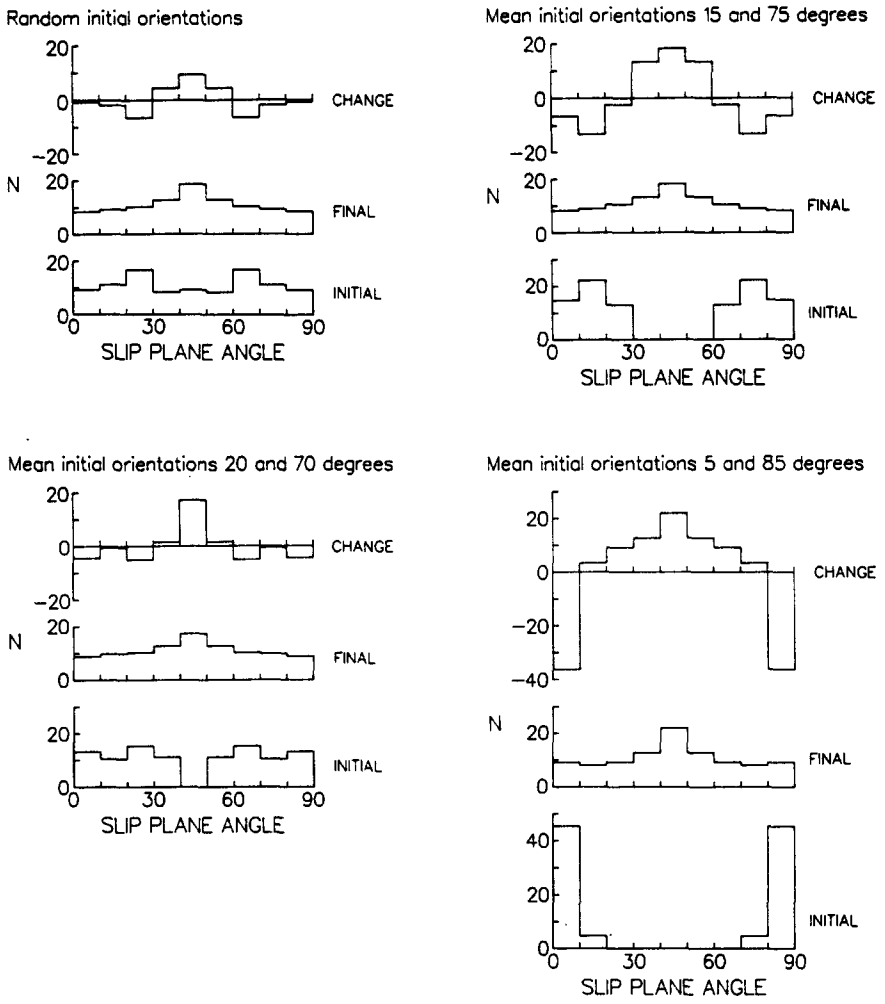

Fig. 5. Histograms of initial and final slip system orientations and difference between initial and final. Angles are measured from horizontal (extension axis) and numbers of orientations N are normalized to sum to 100 for initial and final states.

For several reasons, rigid-body rotations may be smaller in the three-dimensional fabric of real materials than in the finite-element models. Each crystal would be bounded by more than four adjacent crystals, and the demands of compatibility with additional crystals decreases the probability of large rigid-body rotations. However, as seen in Figs. 3 and 4, large lattice rotations, even in the two-dimensional models, occur within crystals, frequently without significant rotation of the crystal as a whole. Rigid-body rotation would also be reduced by grain-boundary sliding, which does not occur in the finite-element models. By allowing slip across grain boundaries, this deformation mechanism allows individual crystals to behave more independently (Etchecopar 1977) and to conform more closely to models of preferred orientation based on non-interacting crystals.

The finite-element models experience preferred orientation of slip planes 45° from the shortening direction (which is also 45° from the extension direction). This rotation is best quantified by considering the angle δ between a slip plane and this 45° orientation. The mean value for these angles will be called δ_i for initial orientations and δ_f for final orientations. Table 1 shows δ_i, δ_f and the difference $\delta_i - \delta_f$ for different initial slip system orientations. The maximum possible δ is 45° and it occurs for a vertical or horizontal slip plane. For a random distribution of slip system orientations, δ_i is half that value, or 22.5°. For mean slip plane angles 20° and 70° from horizontal, δ_i would ideally be 25° (45° minus 20° or 70° minus 45°); δ_is for models with mean slip plane orientations 15° and 75° from horizontal and 5° and 85° from horizontal are 30° and 40°, respectively. The δ_is in Table 1 closely approximate these values. All configurations show a shift of slip planes toward the 45° maximum shear stress orientation (positive $\delta_i - \delta_f$), with the greatest shift occurring in those models with the greatest initial departure from that orientation (Table 1).

Table 1. Initial (δ_i) and final (δ_f) mean slip plane orientations and differences $\delta_i - \delta_f$ between initial and final states for finite-element models. Angles δ_i and δ_f are defined in the text

Initial slip plane orientations	δ_i	δ_f	$\delta_i - \delta_f$
Random	22.5	19.3	3.2
20° and 70° from horizontal	25.0	19.9	5.1
15° and 75° from horizontal	30.0	19.2	10.8
5° and 85° from horizontal	40.0	18.7	21.3

The final angle δ_f is remarkably similar for all initial orientations, as are the final orientation distributions shown in Fig. 5. Net rotations are very small where δ_i is originally close to δ_f (Table 1, random initial orientation), suggesting that this final state represents a relatively stable orientation distribution. Higher strains would probably produce further rotation, but at a greatly reduced rate. Unfortunately, higher strains cannot be achieved in the present finite-element models without excessive element distortion.

If the model proposed above is correct, rigid-body rotation toward the direction of maximum shear stress should be enhanced by a high degree of strength anisotropy. In the finite-element models, elastic strain serves to approximate all the secondary deformation mechanisms present in real crystals. For the low values of τ_f/G in the finite-element models the elastic strains are generally at least several orders of magnitude greater than would occur in real crystals. Therefore, in real crystals most of the strain accommodated elastically in the finite-element models would occur by secondary deformation mechanisms. These mechanisms include glide on slip systems with higher critical resolved shear stress (or lower slip rate at a given stress), dislocation climb, Nabarro–Herring and Coble creep. Although these mechanisms are very crudely represented by elastic behavior, a decrease in elastic shear modulus G (with constant shear strength on the orthogonal slip systems) reduces the dominance of the orthogonal slip systems and produces an effective decrease in strength anisotropy. The effect of this decrease in G is seen in Fig. 6, which shows the initial slip plane configuration and deformed states for τ_f/G ranging from 2.4×10^{-3} to 2.4×10^{-1}. For τ_f/G less than 2.4×10^{-3}, the deformed

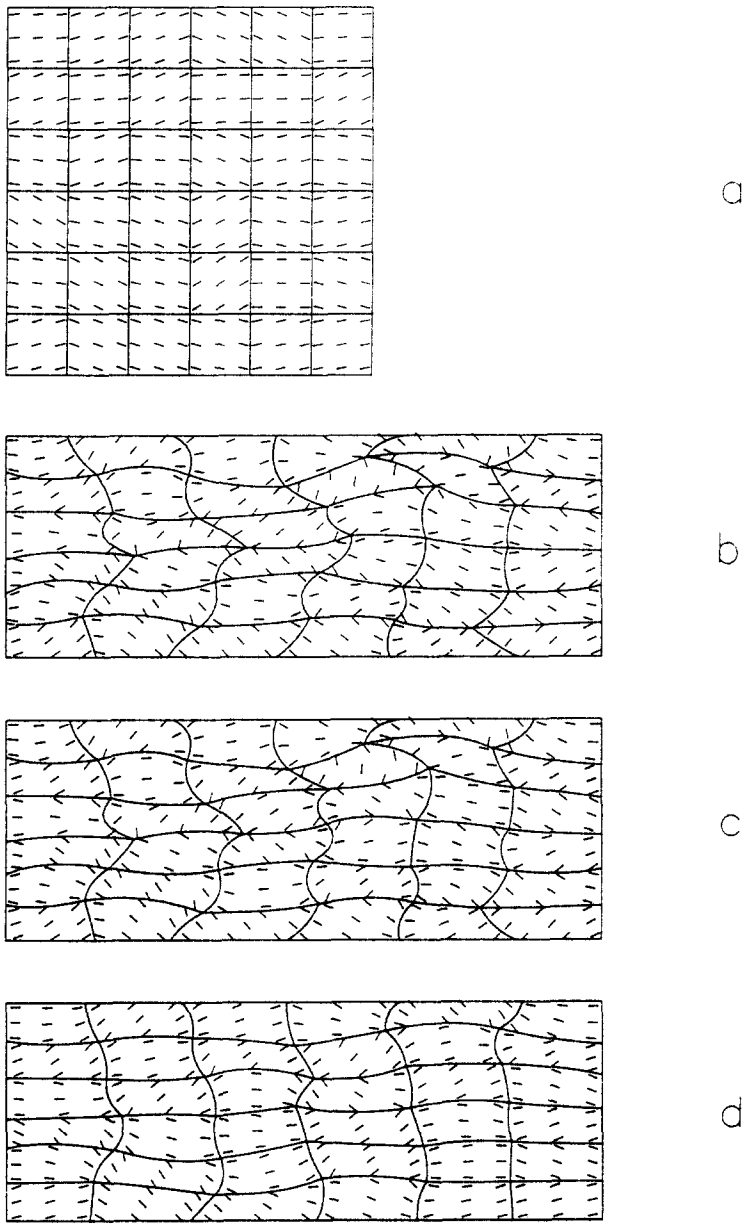

Fig. 6. Initial configuration and deformed configurations for finite-element models with different effective anisotropy. Mean initial dip is 15° for the flat-dipping slip planes (shown) and 85° for the orthogonal steeply dipping slip planes (not shown). All models start with the same slip plane orientation (a), but τ_f/G is 2.4×10^{-3}, 2.4×10^{-2} and 2.4×10^{-1} for models producing the final deformed configurations shown in (b), (c) and (d), respectively.

state is almost identical to that for $\tau_f/G = 2.4 \times 10^{-3}$. For high τ_f/G, strength anisotropy is effectively low and, as expected, deformation is more homogeneous, with less pronounced rigid-body rotations. It is notable, however, that even for $\tau_f/G = 2.4 \times 10^{-1}$, the mean rotation of slip planes towards the orientation of maximum shear stress ($\delta_i - \delta_f$) is 7.3°, not much less than the 10.6° rotation for $\tau_f/G = 2.4 \times 10^{-3}$.

Comparison with rotations for a non-interacting crystal model

Final preferred orientation in finite-element models with orthogonal slip systems is weak. The tendency for reorientation by mechanical interaction may itself be weak, and because the preferred orientation arises from rigid-body rotations imposed by surrounding crystals, this is intrinsically a 'noisy' process that weakens sharply defined preferred orientations. Because the proposed model suggests that rotation of non-slipping crystals into orientations favorable to slip should be expected in all plastically deforming polycrystalline materials, it is desirable to assess the magnitude of this rotation relative to rotations in other types of crystals. Preferred orientation development in the finite-element models is compared to that for a non-interacting crystal model by comparing rotations observed in the finite-element models with those predicted for non-interacting crystals with single slip systems.

To determine rotations for non-interacting crystals, 40% shortening was imposed on crystals with starting slip system orientations corresponding to each of the finite-element models. Each crystal was assumed to have only one slip system, rather than orthogonal systems (which produce no rotation). To represent the orientations for both of an orthogonal pair of slip systems, the number of crystals in each run was double that for the corresponding finite-element model. Shortening strain was applied to each crystal in one thousand equal increments and slip required to produce the shortening was calculated. Incremental rotations were calculated by equation (5), with compensating lattice rotations being equal in magnitude but opposite in sign.

For non-interacting crystals with one slip system, slip planes rotated into positions parallel to the extension direction (perpendicular to the imposed shortening direction). After 40% shortening, the mean rotation toward parallelism with the extension direction was between 25° and 28° for all initial orientation distributions. In contrast, for finite-element models with an initially random fabric, the rotation toward the maximum shear stress orientation was only 3.2° (Table 1). However, as also shown in Table 1, for a high degree of initial preferred orientation in the finite-element models, rotation is nearly comparable in magnitude to the 25–28° rotation for non-interacting crystals with single slip systems. The rotation toward orientations favorable to slip, observed in the finite-element models, would prevent achievement of total parallelism of slip systems, even in a material with only one slip system. In materials that more closely approximate the orthogonal slip system geometry, greater departures from the non-interacting crystal model might be expected.

Other reports of preferred orientation influenced by crystal interaction

It has been reported for metals (Asaro & Needleman 1985), quartz (Tullis *et al.* 1973) and calcite (Wagner *et al.* 1982, Takeshita *et al.* 1987) that for a given strain, observed preferred orientations are weaker than predicted for non-interacting crystals. Of course, this implies only that strain is inhomogeneous, without implying anything about the nature of rotations that result from inhomogeneous deformation. A more systematic perturbation in preferred orientation fabric is caused by bending (curling) of calcite crystals that adopt a plane strain mode of deformation, even when overall deformation of the polycrystalline mass is axisymmetric (Van Houtte *et al.* 1984, Wenk 1985, Wenk *et al.* 1986a). This behavior, first described in metals (Hosford 1964), represents a departure from the homogeneous strain assumed in non-interacting crystal models. The plane strain deformation, taken alone, would result in incompatibility of strain between crystals. The heterogeneous strains and rigid-body rotations that neutralize this incompatibility are analogous to those observed in the finite-element models.

It has also been suggested by several investigators that inhomogeneous strain may cause rotation of slip planes into orientations favorable for slip. This has been observed in simulations of single crystal deformation in ductile metals where strain was localized in slip bands (Needleman *et al.* 1985, Asaro 1985, Lemonds *et al.* 1985). Etchecopar (1974, 1977, 1984) and Etchecopar & Vasseur (1987) numerically simulated deformation of a material with one slip system. Their model allows homogeneous slip within crystals, grain-boundary sliding and rigid-body rotation of crystals. Large gaps and overlaps between adjacent crystals occur, but are minimized. Gapais & Cobbold (1987) have analyzed Etchecopar's data to show that for small strain, grain interaction causes slip planes to rotate into a weak preferred orientation 45° from the shortening direction. This is the same fabric described in this paper; but rather than strengthening as observed in the finite-element models, it weakens with increasing strain and does not persist to the large strains achieved in the finite-element models. Schmid & Casey (1986) also describe rotation into orientations favorable for slip in quartzite undergoing simple shear. This departure from non-interacting crystal theory is attributed to heterogeneous deformation or grain-boundary migration. Whether the phenomena described in these investigations are related to those described in this paper remains unclear.

CONCLUSIONS

In two-dimensional models, a material with two identical, orthogonal slip systems is non-ductile in the

formal von Mises sense. Identical slip must occur on the two systems, and no lattice rotation occurs for any imposed irrotational strain. These characteristics make this material model ideal for study of inhomogeneous deformation and crystal lattice rotation caused by crystal interaction in plastically anisotropic minerals.

As shown, deformation is inhomogeneous both between crystals and within crystals. Interaction between neighboring crystals results in rotation of slip planes into the plane of maximum resolved shear stress (45° to axes of maximum shortening and extension). This preferred orientation is relatively weak and it would only be expected in minerals with similar, nearly orthogonal slip systems. The tendency for rotation of slip planes into orientations favorable to slip should, however, be present in other minerals. It will weaken preferred orientations predicted by non-interacting crystal theory, particularly where the stable preferred orientation is unfavorable for slip.

Acknowledgements—The author is grateful to W. D. Means, M. G. Scarbrough and B. E. Hobbs for their comments and suggestions on an earlier version of this paper.

REFERENCES

Asaro, R. J. 1985. Material modelling and failure modes in metal plasticity. *Mech. Materials* **4**, 343–373.

Asaro, R. J. & Needleman, A. 1985. Texture development and strain hardening in rate dependent polycrystals. *Acta Metall.* **33**, 923–953.

Bishop, J. F. W. 1953. A theoretical examination of the plastic deformation of crystals by glide. *Phil. Mag. Ser.* **7**, 44, 51–64.

Bouchez, J.-L. 1977. Plastic deformation of quartzites at low temperature in an area of natural strain gradient. *Tectonophysics* **39**, 25–50.

Dafalias, Y. F. 1984. The plastic spin concept and a simple illustration of its role in finite plastic transformations. *Mech. Materials* **3**, 223–233.

Etchecopar, A. 1974. Simulations par ordinateur de la déformation progressive d'un aggrégat polycristallin. Etude du dévelopement des structures orientées par écrasement et cisaillement. Unpublished thèse 3e Cycle, Université de Nantes.

Etchecopar, A. 1977. A plane kinematic model of progressive deformation in a polycrystalline aggregate. *Tectonophysics* **39**, 121–139.

Etchecopar, A. 1984. Etude des états de contrainte en tectonique cassante et simulations de déformations plastique (approche mathématiques). Unpublished thèse d'Etat, Université de Montpellier.

Etchecopar, A. & Vasseur, G. 1987. A 3-D kinematic model of fabric development in polycrystalline aggregates: comparisons with experimental and natural examples. *J. Struct. Geol.* **9**, 705–717.

Gapais, D. & Cobbold, P. R. 1987. Slip system domains. 2. Kinematic aspects of fabric development in polycrystalline aggregates. *Tectonophysics* **138**, 289–309.

Gotoh, M. 1978. A finite element formulation for large elastic-plastic deformation analysis of polycrystals and some numerical considerations on polycrystalline plasticity. *Int. J. Numer. Meth. Engng* **12**, 101–114.

Groves, G. W. & Kelly, A. 1963. Independent slip systems in crystals. *Phil. Mag. Ser.* **8**, 877–887.

Hosford, W. F. 1964. Microstructural change during deformation of [011] fiber-textured metals. *Trans. Metall. Soc. AIME* **230**, 12–15.

Knopf, E. B. 1949. Fabric changes in Yule marble after deformation in compression, part I. *Am. J. Sci.* **247**, 433–461.

Kocks, U. F. & Canova, G. R. 1981. How many slip systems, and which? In: *Deformation of Polycrystals: Mechanisms and Microstructures* (edited by Hansen, H., Horsewell, A., Leffers, T. & Lilholt, H.). Riso National Laboratory, Roskilde, Denmark, 35–44.

Law, R. D. 1986. Relationships between strain and quartz crystallographic fabrics in the Roche Maurice quartzites of Plougastel, western Brittany. *J. Struct. Geol.* **8**, 493–515.

Law, R. D., Knipe, R. J. & Dayan, H. 1984. Strain path partitioning within thrust sheets: microstructural and petrofabric evidence from the Moine Thrust zone at Loch Eriboll, northwest Scotland. *J. Struct. Geol.* **6**, 477–497.

Lemonds, J., Asaro, R. J. & Needleman, A. 1985. A numerical study of localized deformation in bi-crystals. *Mech. Materials* **4**, 417–435.

Lin, T. H. 1964. Slip and stress fields of a polycrystalline aggregate at different stages of loading. *J. Mech. Phys. Solids* **12**, 391–408.

Lister, G. S. & Hobbs, B. E. 1980. The simulation of fabric development during plastic deformation: the effects of deformation history. *J. Struct. Geol.* **2**, 355–370.

Lister, G. S. & Paterson, M. S. 1979. The simulation of fabric development during plastic deformation and its application to quartzite: fabric transitions. *J. Struct. Geol.* **1**, 99–115.

Lister, G. S., Paterson, M. S. & Hobbs, B. E. 1978. The simulation of fabric development in plastic deformation and its application to quartzite: the model. *Tectonophysics* **45**, 107–158.

Lister, G. S. & Williams, P. F. 1983. The partitioning of deformation in flowing rock masses. *Tectonophysics* **92**, 1–33.

Mancktelow, N. S. 1981. Strain variation between quartz grains of different crystallographic orientation in a naturally deformed metasiltstone. *Tectonophysics* **78**, 73–84.

Needleman, A., Asaro, R. J., Lemonds, J. & Peirce, D. 1985. Finite element analysis of crystalline solids. *Comput. Meth. appl. Mech. Engng* **52**, 689–708.

Nicolas, A. & Poirier, J. P. 1976. *Crystalline Plasticity and Solid State Flow in Metamorphic Rocks*. John Wiley and Sons, London.

Paterson, M. S. 1969. The ductility of rocks. In: *Physics of Strength and Plasticity* (edited by Argon, A. S.). The Orowan 65th Anniversary Volume, MIT Press, 377–392.

Price, G.-P. 1985. Preferred orientations in quartzites. In: *Preferred Orientations in Deformed Metals and Rocks* (edited by Wenk, H.-R.). Academic Press, New York, 385–406.

Rutter, E. H. & Rusbridge, M. 1977. The effect of non-coaxial strain paths on crystallographic preferred orientation development in the experimental deformation of marble. *Tectonophysics* **39**, 73–86.

Schmid, S. M. & Casey, M. 1986. Complete fabric analysis of some commonly observed quartz c-axis patterns. In: *Mineral and Rock Deformation: Laboratory Studies* (edited by Hobbs, B. E. & Heard, H. C.). *Am. Geophys. Un. Geophys. Monogr.* **36**, 263–286.

Takeshita, T., Tome, C., Wenk, H.-R. & Kocks, U. F. (1987) Single-crystal yield surface for trigonal lattices: application to texture transitions in calcite polycrystals. *J. geophys. Res.* **92**, 12,917–12,930.

Taylor, G. I. 1938. Plastic strain in metals. *J. Inst. Metals* **62**, 307–324.

Tharp, T. M. 1985a. A program to evaluate the ductility of minerals. *Comput. Geosci.* **11**, 85–89.

Tharp, T. M. 1985b. Numerical models of subduction and forearc deformation. *Geophys. J. R. astr. Soc.* **80**, 419–437.

Timoshenko, S. P. & Goodier, J. N. 1970. *Theory of Elasticity* (3rd edn). McGraw-Hill, New York.

Tullis, J. A., Christie, J. M. & Griggs, D. T. 1973. Microstructures and preferred orientations of experimentally deformed quartzites. *Bull. geol. Soc. Am.* **84**, 297–314.

Turner, F. J. & Ch'ih, C. S. 1951. Deformation of the Yule Marble: part III—observed fabric changes due to deformation at 10,000 atmospheres confining pressure, room temperature, dry. *Bull. geol. Soc. Am.* **62**, 887–906.

Urai, J. L., Means, W. D. & Lister, G. S. 1986. Dynamic recrystallization of minerals. In: *Mineral and Rock Deformation: Laboratory Studies* (edited by Hobbs, B. E. & Heard, H. C.). *Am. Geophys. Un. Geophys. Monogr.* **36**, 161–199.

Van Houtte, P. & Wagner, F. 1985. Development of textures by slip and twinning. In: *Preferred Orientation in Deformed Metals and Rocks: An Introduction to Modern Texture Analysis* (edited by Wenk, H.-R.). Academic Press, Orlando, 233–258.

Van Houtte, P., Wenk, H.-R. & Wagner, F. 1984. The curling effect as a possible explanation of the uniaxial compression textures of calcite. In: *Proceedings of the 7th International Conference on Textures of Materials*, 153–158.

von Mises, R. 1928. Mechanik der plastischen Formanderung von Kristallen. *Z. angew. Math. Mech.* **8**, 161–185.

Wagner, F., Wenk, H.-R., Kern, H., Van Houtte, P. & Esling, C. 1982. Development of preferred orientation in plane strain deformed limestone: experiment and theory. *Contr. Miner. Petrol.* **80**, 132–139.

Wagner, F., Wenk, H.-R., Kern, H., Van Houtte, P. & Esling, C. 1984. Evolution of deformation textures in calcite. In: *Proceedings of the 7th International Conference on Textures of Materials*, 165–171.

Wenk, H.-R. (editor) 1985. Carbonates. In: *Preferred Orientation in*

Deformed Metals and Rocks. Academic Press, New York, 361–384.
Wenk, H.-R., Kern, H., Van Houtte, P. & Wagner, F. 1986a. Heterogeneous strain in axial deformation of limestone, textural evidence. In: *Mineral and Rock Deformation: Laboratory Studies* (edited by Hobbs, B. E. & Heard, H. C.). *Am. Geophys. Un. Geophys. Monogr.* **36**, 287–295.
Wenk, H.-R., Takeshita, T., Van Houtte, P. & Wagner, F. 1986b. Plastic anisotropy and texture development in calcite polycrystals. *J. geophys. Res.* **91**, 3861–3869.
Wenk, H.-R., Venkitasubramanyan, C. S. & Baker, D. W. 1973. Preferred orientation in experimentally deformed limestone. *Contr. Miner. Petrol.* **38**, 81–114.
Zienkiewicz, O. C. 1971. *The Finite Element Method in Engineering Science*. McGraw-Hill, London.